USING HIGH-RESOLUTION GPS TRACKING DATA OF BIRD FLIGHT FOR METEOROLOGICAL OBSERVATIONS

by Jelle Treep, Gil Bohrer, Judy Shamoun-Baranes, Olivier Duriez, Renato Prata de Moraes Frasson, and Willem Bouten

Griffon vulture in flight carrying a UvA-BiTS GPS logger. This image provides a clear visualization of the current state of tracking soaring birds with GPS. Photo courtesy of Christian Aussaguel.

High-resolution GPS tracks of soaring birds can be used to estimate wind velocity and convective velocity scale and thereby contribute to high-resolution weather observations.

Biologging is being used increasingly to track moving organisms in space and time (Ropert-Coudert and Wilson 2005; Rutz and Hays 2009; Bouten et al. 2013; Dodge et al. 2013). As tags become lighter, cheaper, and more efficient, there is a rapidly growing amount of fine-resolution data being collected. Besides increasing data volumes, further sophistication of the GPS tags also yields different types of data in addition to location (e.g., acceleration, compass direction, temperature, pressure). Many studies have investigated the influence of meteorology, ocean currents, and the distribution of food on foraging and migration movement patterns (e.g., Dragon et al. 2010; Sapir et al. 2011; Shamoun-Baranes et al. 2011; Bohrer et al. 2012; Safi et al. 2013; Dodge et al. 2014). This is done by annotating remote sensing, ground station, and reanalysis datasets to the observed locations of the animals from biologging following the track annotation approach (Mandel et al. 2011). Knowledge of the environmental conditions during movement is needed to improve the understanding of the animals' movement ecology and to develop predictive models of their movement (Nathan et al. 2008). Beyond providing richer and more accurate information about the animals' locations during movement, the wealth of available high-resolution information offers new possibilities of estimating environmental ▶

conditions directly from the data collected on the tag (Charrassin et al. 2008). This can be fruitful for determining the values of environmental variables that are otherwise hard to measure. For example, measurements of boundary layer properties, such as thermal structures, are scarce, especially in remote and mountainous locations. In this paper we demonstrate an approach for using GPS data of soaring birds to observe atmospheric boundary layer properties.

BIRD FLIGHT IS STRONGLY RELATED TO METEOROLOGICAL CONDITIONS.

Many large birds use soaring and gliding flight because flapping flight is energetically more costly (Hedenstrom 1993; Sakamoto et al. 2013; Duriez et al. 2014). Birds that use thermal convection for soaring use the energy in buoyant warm air to gain altitude and then use the potential energy to glide to the next thermal (Van Loon et al. 2011) (Fig. 1; a dynamic visualization can be found at www.doarama.com/view/433747). This type of flight will therefore be affected by the intensity of surface sensible heat flux and the atmospheric boundary layer depth, which determine the strength and altitude range of available thermal uplift (Shannon et al. 2002a; Shamoun-Baranes et al. 2003b; Mandel et al. 2008). Several species use orographic uplift instead, thereby gliding for kilometers along mountain ridges (Shepard et al. 2011; Bohrer et al. 2012). As a result of a low wing loading, soaring birds can be extremely effective when making use of thermals (Pennycuick 1971; Spaar and Bruderer 1996), lowering their sink rate relative to air to velocities on the order of 1 m s^{-1} (Pennycuick 1971).

AFFILIATIONS: Treep, Shamoun-Baranes, and Bouten—Computational Geo-Ecology, IBED, University of Amsterdam, Amsterdam, Netherlands; Bohrer and de Moraes Frasson—Department of Civil, Environmental and Geodetic Engineering, The Ohio State University, Columbus, Ohio; Duriez—CEFE UMR 5175, CNRS - Université de Montpellier - Université Paul-Valéry Montpellier - EPHE, Montpellier, France
CORRESPONDING AUTHOR: Jelle Treep, Institute of Environmental Biology, Utrecht University, Padualaan 8, 3584 CH, Utrecht, Netherlands
E-mail: h.j.treep@uu.nl

The abstract for this article can be found in this issue, following the table of contents.
DOI:10.1175/BAMS-D-14-00234.1

In final form 17 September 2015

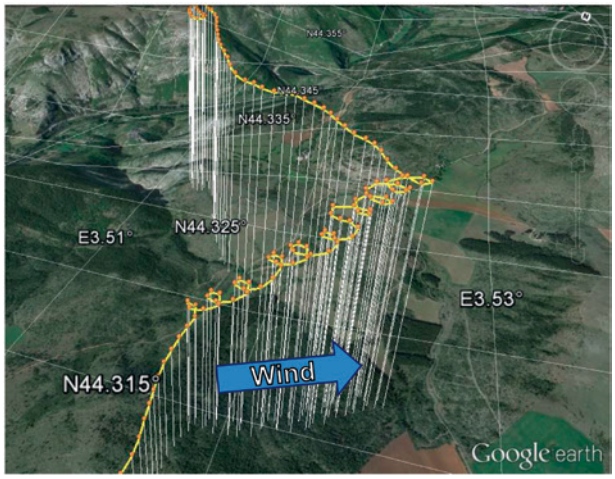

Fig. 1. GPS sequences of a griffon vulture on 2 Aug, uploaded from Google Earth. With circling flight, the vulture gains altitude in a thermal without flapping, after which it continues gliding toward its intended destination. During circling, there is a net horizontal drift that is caused by horizontal advection of the thermal due to wind. The blue arrow indicates the estimated wind direction based on this horizontal drift.

In addition to vertical wind, horizontal wind speed and direction also influence the flight patterns of soaring birds (Shamoun-Baranes et al. 2003a; Mandel et al. 2008; Lanzone et al. 2012; Vansteelant et al. 2014). Wind can displace birds while they are gliding as well as during the climbing phase as thermals are horizontally advected by wind (Kerlinger and Gauthreaux 1984; Kerlinger 1989).

Birds' flight patterns have been used for gathering qualitative information about thermals for a long period of time (Huffaker 1898; Woodcock 1940). However, obtaining quantitative information remained difficult until the invention of small altimeters and GPS devices. Shannon et al. (2002b) showed that birdborne data can be used for obtaining quantitative meteorological observations. In their study, white pelicans *(Pelecanus erythrorhynchos)* were equipped with altimeters and tracked from the ground during cross-country flight. They demonstrated that the altimeter data could be used to estimate thermal updraft intensities over both valleys and mountainous areas. With the miniaturization of current GPS devices, with a temporal sampling frequency that can be set to higher than 1 Hz, both the quantity and accuracy of data points have greatly improved (Lanzone et al. 2012; Bouten et al. 2013) and opportunities are created to obtain more extensive meteorological information from bird-flight data.

Measurements of microscale meteorological processes are mostly obtained from static in situ or remote

sensors, such as anemometers, temperature, pressure, and humidity sensors, which provide time series at one point in space. Multiple sensors are needed to capture the horizontal and vertical heterogeneity in the boundary layer. Platforms such as towers and radiosondes with static sensors, or remote sensing methods such as lidar, can be used to obtain vertical profiles. Horizontal heterogeneity can best be captured with flying platforms, such as aircrafts, balloons, or unmanned aerial vehicles (UAVs) (Stull 1988). UAVs have improved greatly in size and efficiency in recent times; however, they are still costly to operate, both in funds and labor. Recent papers have highlighted the potential of using smartphone and vehicle-based pressure and temperature observations for improved high-resolution weather analysis and prediction (Mahoney and O'Sullivan 2013; Mass and Madaus 2014). We propose that airborne data from birds could be complementary to these data sources, particularly in remote areas and mountainous regions, where UAV access is difficult and smartphones and vehicles are not abundant.

By now, billions of GPS data points have been collected from birdborne tags worldwide. A substantial amount of such data are available in online databases, such as Movebank (www.movebank.org) and the University of Amsterdam Bird Tracking System (UvA-BiTS; www.uva-bits.nl), and the type of data ranges from very local foraging flights to global-scale migratory movements. In this study we explore the potential of using 3D location data of griffon vultures *(Gyps fulvus)* for estimating wind velocity and the convective velocity scale. The convective velocity scale is a scaling variable that can be used to estimate the strength of thermally driven uplift and is used in convective mixed-layer similarity theories (Stull 1988). The variables needed to estimate it are rarely observed by meteorological ground stations.

ESTIMATION OF WIND VELOCITY AND CONVECTIVE VELOCITY SCALE FROM THREE-DIMENSIONAL GPS LOCATION DATA. During soaring flight a bird typically circles upward in a thermal (climbing phase) and then glides and loses altitude to make horizontal progress in a particular direction (Fig. 1). During the climbing phase a bird may drift from the main flight bearing. This drift is caused by the horizontal displacement of thermals by advection with the horizontal wind (Kerlinger and Gauthreaux 1984; Stull 1988). In our study, we use this horizontal displacement of the thermal over time to estimate wind velocity. We developed an algorithm to automatically classify circling bouts (periods of consecutive circling behavior), which can handle the large datasets of high-resolution GPS locations over hours, days, or even years of flight. Periods of circling and gliding can be distinguished because they show different characteristic combinations of climb rate, ground speed, and flight direction variation (Fig. 2). Further details about the classification algorithm can be

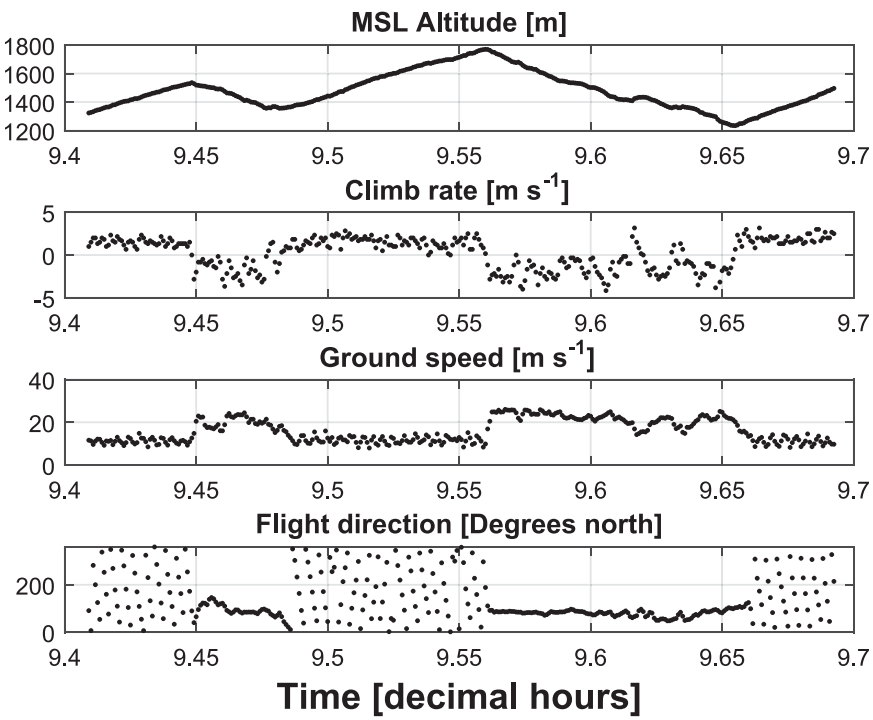

Fig. 2. Time series of altitude (m MSL), climb rate (m s^{-1}), ground speed (m s^{-1}), and flight direction of a griffon vulture between 0924 and 0942 UTC 2 Aug 2012. Two distinct types of behavior can be distinguished in all variables, namely circling flight and gliding flight. During circling flight, the vulture is gaining altitude; thus, the climb rate is positive, the horizontal speed is relatively low (between 10 and 15 m s^{-1}), and the direction is continuously changing. During gliding, the vulture is mainly losing altitude, the climb rate is mainly negative, the horizontal speed is relatively high, and the direction constant or gradually changing.

found in the appendix. We estimated the horizontal displacement of each thermal with linear regression through all GPS points in each circling bout. The net horizontal displacement of the bird divided by the time span of each circling bout yields an estimate for wind speed. The direction of the horizontal displacement yields an estimate for wind direction. Estimates of wind velocity from longer periods of circling suffer less from uncertainty that is introduced by variation in the horizontal position because of the circling movement. Therefore, we selected only circling bouts that took at least 72 s for our analyses.

For estimations of vertical wind velocities in a thermal, we used data from the same circling bouts. Circling flight is particularly suitable for estimating vertical air velocity because birds try to minimize sink rate relative to the upward-moving air in order to gain altitude. Thus, average sink rate estimations are more accurate when predicted from circling flight than from gliding flight. The sink rate of a bird relative to the air can be estimated using the theoretical formulation of aerodynamics of soaring birds, which has been established based on wind tunnel experiments and field observations (Pennycuick 1971; Tucker 1987). The sink rate is mainly dependent on morphological characteristics and the horizontal airspeed of the bird. We estimated the airspeed of the vultures from its ground speed vector by subtracting the wind velocity. For this wind velocity we used the estimates from the horizontal displacement of thermals. As we explained earlier, these estimates for the horizontal wind speed from the GPS locations are independent of sink rate. The vertical wind velocity is estimated from the sink rate added to the measured climb rate between two GPS fixes (Shannon et al. 2002b). All equations can be found in the appendix to this paper.

CASE STUDY: GRIFFON VULTURES IN GRANDS CAUSSES. Since 2010, 22 griffon vultures from a colony in the Grands Causses area, southern France, were equipped with GPS tags from the UvA-BiTS system (Bouten et al. 2013) in order to study their foraging behavior [see additional details in Monsarrat et al. (2013)]. The solar-powered GPS tags weigh about 45 g and contain a triaxial accelerometer, rechargeable battery, datalogger, and a two-way communication system, which makes it possible to remotely download data and change the measurement interval (Bouten et al. 2013). The position and altitude errors of the UvA-BiTS devices have been shown to be in line with other GPS systems. In a stationary position, and with a measurement interval of 6 s, the mean position error is 1.42 m (90% contour interval is [0.2, 2.33]) and the mean altitude error is 1.42 m (90% contour interval is [0.25, 3.75]).

The Grands Causses area is characterized by deep canyons (of approximately 400-m depth) in between limestone plateaus along the rivers Tarn and Jonte (Fig. 3). The nests of the griffon vultures are located on steep cliffs along the canyons. The land is mainly used for extensive sheep farming (grazing in steppe meadows) and for forestry *(Pinus sylvestris)*. The area has a dry and sunny Mediterranean climate. The home range of this resident griffon vulture population is located within a radius of roughly 50 km around the main colonies (global home range area used by all birds approaches 10,000 km^2) (Monsarrat et al. 2013). According to accelerometer data, griffon vultures almost exclusively use circling and gliding flight and flap only very rarely, typically at takeoff (Shepard

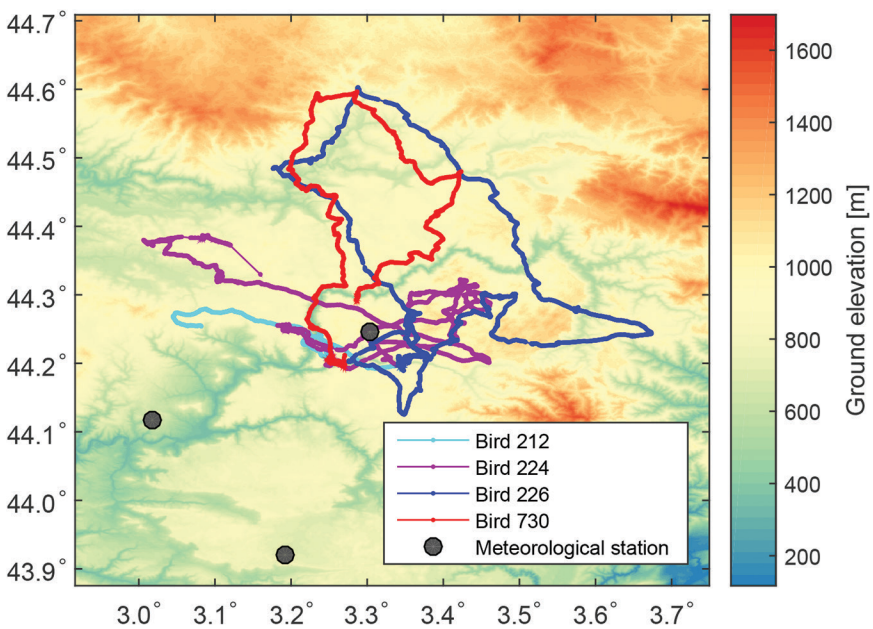

Fig. 3. Topographic map of the area combined with GPS tracks of four griffon vultures on 2 Aug 2012 (lines) and the locations of three meteorological stations.

Table 1. Flight characteristics for four individual vultures that have been tracked with high-resolution GPS on 2 Aug 2012. Standard deviations are given in parentheses.

Individual	Flight times (UTC)	Distance covered (km)	No. of circling sequences (>72 s)	Avg climb rate (m s^{-1})	Avg sink rate (m s^{-1})	Avg circling radius (m)	Max altitude in a thermal (km MSL)
212	1200–1230	26.4	3	2.4 (0.89)	1.33 (0.65)	21.3 (3.84)	1.27 (0.04)
	1420–1445	13.0					
	1700–1720	15.5					
224	0730–1145	189.3	27	1.3 (0.74)	1.10 (0.79)	23.4 (4.47)	1.38 (0.26)
	1425–1630	95.7					
	1745–1800	8.3					
226	0800–1230	245.9	29	2.0 (1.06)	1.06 (0.32)	21.7 (5.80)	1.57 (0.28)
	1500–1620	58.1					
730	0825–1140	157.4	20	1.8 (0.77)	0.91 (0.14)	25.5 (4.13)	1.32 (0.24)

et al. 2011; Duriez et al. 2014). They fly mostly during sunny days, when convection in the atmospheric boundary layer provides abundant thermal uplift. For this case study the measurement interval of four loggers was set to 3 s. Data were collected on 2 August 2012 from four birds tracked simultaneously. Three of the four vultures were mainly active in the morning making long flights. All four vultures made a few shorter flights in the afternoon (see Table 1 for further flight details). During that day, we recorded 79 circling bouts that were longer than 72 s and hence 79 estimates of wind velocity. On 2 August 2012 the weather was warm and sunny with a maximum temperature of 28.3°C. The wind increased from around 3 m s^{-1} in the morning from various directions to 7 m s^{-1} from the northwest (ground station data).

For evaluation of our GPS estimates of wind speed and direction we used hourly data obtained from three meteorological stations (owned by Météo-France), located on high vantage points within the home ranges of the griffon vultures [Millau-Soulobres (44.118°N, 3.018°E; 714 m), Saint-Pierre-des-Tripiers (44.245°N, 3.303°E; 929 m), and La Cavalerie (43.921°N, 3.192°E; 718 m)]. The sensors for wind are located at 10 m above the surface. Figure 3 shows a topographic map of the region, the locations of the meteorological stations, and the GPS tracks of the four vultures on 2 August 2012. We interpolated the ground station data in space and time to the latitude, longitude, and time stamps of the GPS measurements. For spatial interpolation to the location of the bird we used weighted distance interpolation. We compared wind speed estimates with ground station data using Pearson's correlation and for wind direction we used a correlation coefficient for directional data ρ_{cc} (Berens 2009).

The global Ocean–Land–Atmosphere Model (OLAM; Walko and Avissar 2008) was used to evaluate the GPS estimates of vertical velocity of air. In any atmospheric model, the vertical wind speed averages to zero at a spatial scale that is larger than a few hundreds of meters, or in observations over a time period longer than about 30 min. Meteorological stations, which report hourly averages, therefore, do not report mean vertical wind speed. Similarly, regional meteorological models that use a resolution coarser than hundreds of meters (typically several kilometers) cannot resolve vertical wind that is associated with thermal convection, while thermals are very complex structures, where turbulent fluctuations can be larger than the mean uplift strength (Lenschow and Stephens 1980). Instead, they use different parameterizations to estimate the convective tendencies in the atmospheric boundary layer, such as the convective velocity scale (Stull 1988). If the birdborne GPS estimates of vertical velocity would provide a random sample from the thermal column, the average of all points in a thermal would be a direct estimate of the mean uplift strength in a thermal, which scales with convective velocity scalea w_*. However, as the birds try to optimize their climb rate by mainly flying in the fast-rising sections of the thermal, but are constrained to flying in circles in order to minimize their banking angle and sink rate (Shepard et al. 2013), and potentially also by selecting the larger thermals, birdborne observations cannot be treated as an unbiased random sample of mean uplift strength. Therefore, the two variables (observed vertical wind and modeled w_*) may have a different mean value range. Nonetheless, despite the relative bias of the means, they are expected to strongly correlate in space and time.

OLAM was initialized with weather reanalysis data from the European Centre for Medium-Range Weather Forecasts (ECMWF) interim reanalysis dataset (Dee et al. 2011; data available online at http://apps.ecmwf.int/datasets/). A geodesic atmospheric grid is built from spherical hexagonal elements. The atmospheric grid is gradually refined around the area of interest, producing a fine grid resolution of 300 m over a circular area of 30 km in diameter. The vertical grid extends upward, from the surface to 25 km in height. The vertical resolution is 30 m near the surface and becomes gradually coarser with altitude to 1600 m for the uppermost layer. Fine-resolution maps of surface elevation [Shuttle Radar Topographic Mission 90-m resolution; NASA (2012)] and land-cover [Coordinated Information on the Environment (CORINE) land-cover facility 100-m resolution; EEA (2006)] data are used as model input. Output is generated every 30 min. The convective velocity scale is calculated from the sensible heat flux H, boundary layer height z_i, and boundary layer average potential temperature $\bar{\theta}$:

$$w_* = \left[\frac{g z_i H}{\rho c_p \bar{\theta}} \right]^{1/3}, \qquad (1)$$

where ρ is the air density and c_p is the specific heat at constant pressure. The contribution of water-vapor flux to w_*, which is typically small in convective boundary layers, is neglected. Sensible heat flux and potential temperature are resolved by OLAM, and boundary layer height is parameterized in OLAM.

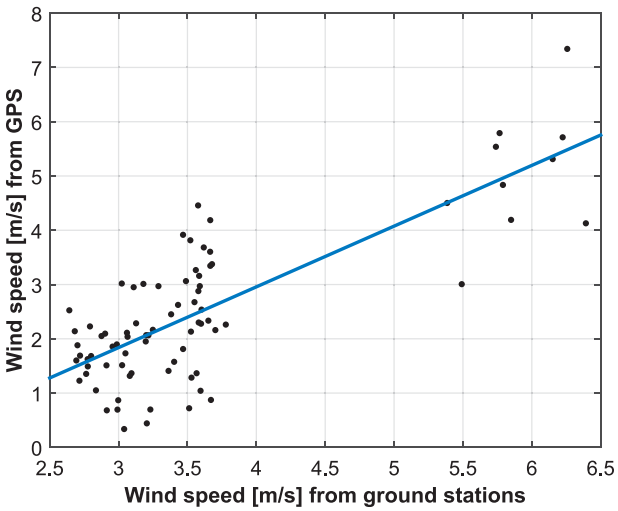

Fig. 4. GPS estimates of wind speed as a function of ground station measurements of wind speed at 10 m AGL. Ground station measurements from three ground stations are interpolated in space and time to the location of the GPS estimates. Pearson's *r* is 0.78 (*p* < 0.001).

RESULTS. GPS estimates of wind speed and direction are significantly and positively correlated with ground station data (Pearson's $r = 0.78$; $p < 0.001$ for wind speed and $\rho_{cc} = 0.67$; $p < 0.001$ for wind direction). Wind speed measurements from ground station data have higher values than the estimates from the GPS tracking data (Fig. 4). In the lower wind speed ranges (4–7 m s^{-1} along the x axis), there is larger variation in the wind speed estimates from GPS than in the ground station data. A main reason for this variation could be that our GPS estimates provide 79 independent observations of wind speed from a range of altitudes (Fig. 7), compared to 12 hourly observations from the ground stations from which 79 data points are derived by interpolation. An additional source of mismatch between wind speed measured by the ground stations and estimated by the birds can be the effect of local topography around the meteorological station, especially in areas of complex terrain, which can result in very localized differences in wind speeds. The overall distributions of wind directions from GPS and ground station data are similar with winds coming from a west-to-northwest direction (Fig. 5); however, there is a systematic bias. The ground station observations of wind direction range from west to north whereas the GPS data range from southwest to northwest. This turning in wind direction with height is consistent with the Ekman wind profile (Stull 1988).

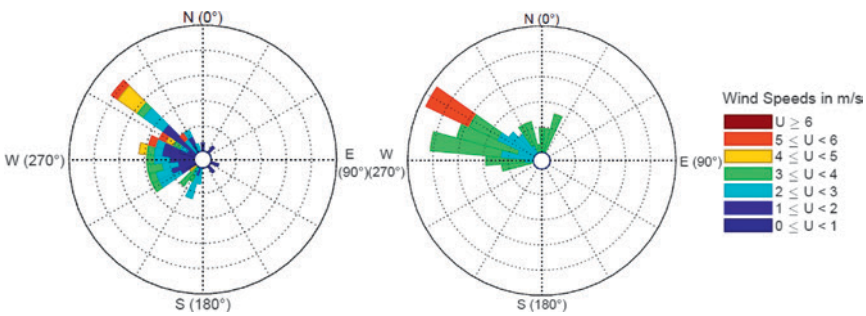

Fig. 5. Wind roses on 2 Aug 2012 estimated from (left) GPS data of griffon vultures and (right) hourly ground station data at 10-m altitude linearly interpolated in time to the time stamps of the GPS estimates. The directional correlation between the GPS estimates of wind direction and ground station measurements is ρ_{cc} = 0.67 (p < 0.001).

The estimated mean vertical wind speed in the

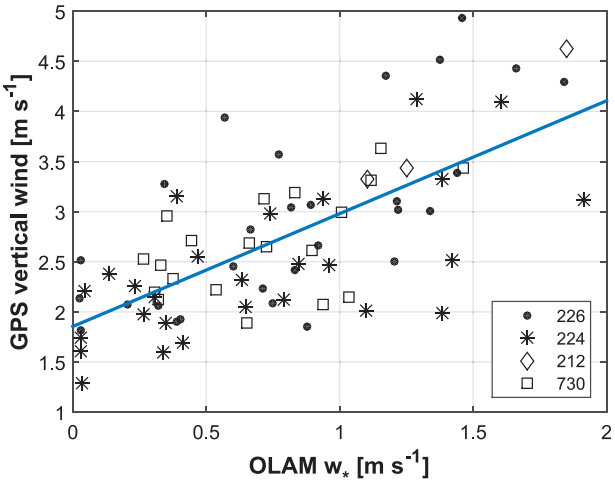

Fig. 6. Average vertical wind in circling bouts as a function of convective velocity scale calculated from OLAM model output. Half-hourly OLAM output is interpolated in space and time to the locations of the GPS estimates. Pearson's *r* is 0.69 ($p < 0.001$).

convective updrafts where vultures circle is significantly correlated with w_* calculated from OLAM output (Pearson's $r = 0.69$; $p < 0.001$). To test if the individual vulture has a significant effect on our vertical wind speed estimates, we used a generalized linear mixed model with w as the response variable, w_* from OLAM as the predictor variable, and individual as a random factor. We found that individual random effects are not significant (all $p > 0.05$), and w is positively and significantly correlated with w_* ($R^2 = 0.46$; $\beta = 1.12$; $p < 0.001$). This suggests that vertical wind estimates are consistent among individuals. While direct measurements of vertical wind from other sources are not available, the high correlation between our vertical wind estimates and the model's w_* indicates that GPS data can be used to estimate vertical wind velocity (Fig. 6). Mean vertical wind, as estimated from the flight tracks, increases around midday and follows a temporal diurnal pattern that agrees with boundary layer theory of increasing updraft intensities and growth of the boundary layer starting with solar radiation in the morning and intensifying during the day followed by a decline phase in the late afternoon and toward the evening (Fig. 7). Similarly, in the first hours after sunrise the maximum flight altitudes increase, which agrees with the diurnal pattern of boundary layer height; however, the increase does not continue until midday (Fig. 7). Around midday, the three vultures that were flying stopped for feeding or to rest (Table 1), which is a possible explanation for the vultures not climbing to the maximal potential elevation.

CONCLUSIONS. Integrating meteorological and biological expertise has great potential for both communities (Charrassin et al. 2008; Shamoun-Baranes et al. 2010; Shepard et al. 2011). This study shows that high-resolution GPS measurements of avian flight behavior can be used to collect information about meteorological conditions at a finescale and in areas where sensors are not available. Soaring birds, such as griffon vultures, are very efficient when circling in thermals (Pennycuick 1971; Shannon et al. 2002b) and therefore provide unique measurements of vertical velocities in thermals. The strong correlation of the mean vertical velocity in a thermal with a model-resolved convective velocity scale is not surprising given mixed-layer similarity theory (Stull 1988). The correlation shows that the birdborne observations provide useful information of updraft intensities at the temporal and spatial scales of the model output. Since we compare the estimates with model data at half-hourly time intervals and spatial averages over grid cells of 300 m, it is hard to evaluate the accuracy of individual observations. The variation

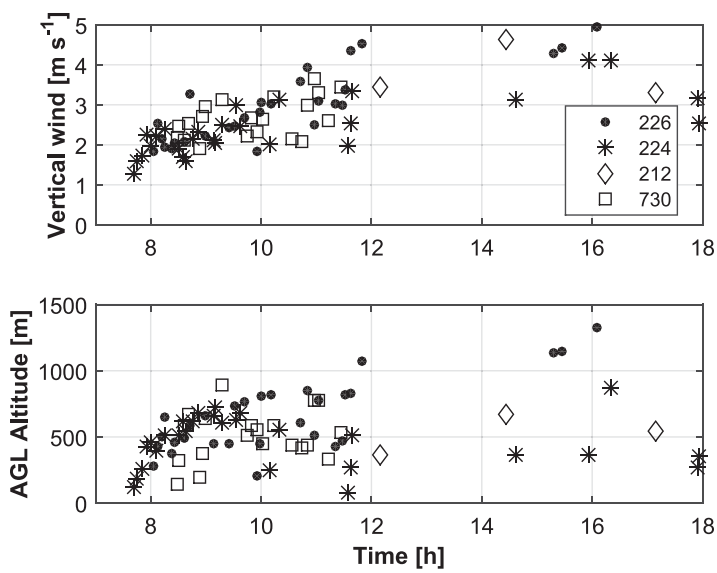

Fig. 7. (top) Mean vertical wind in a thermal estimated from GPS data of griffon vultures as a function of time of day and (bottom) maximum flight altitude (m AGL) reached in each thermal as a function of time of day. Altitude is determined by subtracting the ground-level elevation (extracted from the SRTM 90 elevation dataset) from the altitude of the bird (m MSL), measured by the GPS. Different symbols represent different individuals. On the day of data collection, the griffon vultures were mainly active in the morning.

in GPS estimates could be caused by uncertainties in our method or the GPS estimates might be more informative than the model data. The same is true for estimates of wind velocities, which correlate well with ground station data, both when it comes to speed and direction. No collocated data are available to test the accuracy in detail, so we can only speculate about the causes of the different velocity ranges and the increased variation in the GPS estimates compared to ground station data. A better validation may be performed by extrapolating the ground station data to the altitude of the bird using radix-layer similarity theory (Santoso and Stull 2001) and accounting for the effects of mechanical stress and thermal wind on the variation of wind direction with altitude. For this, reliable data sources of convective velocity scale, boundary layer height, geostrophic winds, and temperature gradients are needed at fine resolution. The lack of finescale weather data for evaluation makes it difficult to validate our measurements. Individual estimates of climb rate are fairly consistent, which suggests that they can be used individually to map thermals at even finer temporal and spatial scales. However, until the development of an observation platform that could obtain direct measurements of uplift and wind speed over a full-thermal volume, rather than at a point, we could not know for certain in which part of the thermal the bird is located; we can only compare relative differences in climb rates.

A good understanding of the relations between bird movements and meteorology is crucial to enhancing meteorological information content. These interactions can be very specific for different species, but also could depend on the flight objective of the bird—for example, whether a bird is searching for food, commuting between roosts, or traveling to migrate (Shepard et al. 2011). When soaring birds travel large distances, they can reduce their energy expenditure by circling in the stronger updrafts of the middle part of the boundary layer (Shannon et al. 2002a; Shamoun-Baranes et al. 2003b; Sapir et al. 2011). When searching for food or commuting between roosts, altitude plays a less prominent role since prey may be harder to detect at higher altitudes or climbing to high altitudes is not necessary if nearby targets are within gliding range.

Further miniaturization of GPS tags, batteries, and sensors in the future will likely yield an exponential growth of high-resolution data in the coming years. If knowledge of relations between bird flight and finescale meteorology are improved, more and more accurate information can be obtained. High-resolution GPS data from birds can therefore become a promising complementary data source, filling gaps in conventional observation systems (Charrassin et al. 2008). Potential products can be used by glider pilots, in air quality forecasting, and for emergency management in the case of chemical releases. By contributing data and expertise, biologists can help improve meteorological products, which in turn can be used to help understand how birds respond to dynamic atmospheric conditions at these finescales. The key perhaps is beginning an open dialogue between these communities, and we hope that the current study will help stimulate future collaboration.

ACKNOWLEDGMENTS. Our tracking studies are facilitated by infrastructures for e-Science, developed with support of the NLeSC (www.esciencecenter.com/) and LifeWatch, carried out on the Dutch national e-infrastructure with the support of the SURF Foundation. We acknowledge the support provided by COST–European Cooperation in Science and Technology through the Action ES1305 "European Network for the Radar Surveillance of Animal Movement" (ENRAM). The simulations of the Ocean–Land–Atmosphere Model have been performed at the Ohio Supercomputer Center. GB and RPdMF were funded in part by National Science Foundation Grant IOS-1145952 and NASA Grant NNX11AP61G. We thank the staff from LPO Grands Causses (T. David, P. Lécuyer, B. Eliotout, R. Neouze, and M. Terrasse) and the Parc National des Cevennes (B. and S. Descaves, J. Pinna, and I. Malafosse) for their assistance in the field. The tracking of griffon vultures with GPS was funded by ANR project SOFTPOP, coordinated by F. Sarrazin and C. Bessa-Gomes. The wind speed and direction data for this work have been provided by Météo-France. We are grateful to G. Young and two anonymous reviewers for discussion and constructive feedback on earlier versions of the manuscript.

APPENDIX: METHODS FOR DERIVING INFORMATION FROM GPS TRACKS.

Classification of circling bouts. To classify circling bouts in the data, we use ground speed, the flight direction, and the climb rate of the bird. We estimate the ground speed V_i (m s^{-2}) at a location P_i by averaging the speed of the trajectory that ends at this location (P_{i-1} minus P_i) and the trajectory that starts at this location (P_i minus P_{i+1}):

$$V_i = \frac{[(P_i - P_{i-1})/(t_i - t_{i-1})] + [(P_{i+1} - P_i)/(t_{i+1} - t_i)]}{2}, \quad \text{(A1)}$$

where t_i is the time stamp of GPS data point i. The horizontal flight direction at a location is the average of the bearing of two lines connecting the trajectory

that ends at this location and the trajectory that starts at this location. The climb rate V_c (m s^{-1}) is obtained in the same manner as the ground speed. First, the climb rates in between the locations are calculated by dividing the altitude z (m) difference by the time interval. Then, the climb rate at a location is obtained by averaging the climb rate of the trajectory that ends at this location and the trajectory that starts at this location:

$$V_c = \frac{[(z_i - z_{i-1})/(t_i - t_{i-1})] + [(z_{i+1} - z_i)/(t_{i+1} - t_i)]}{2}. \quad \text{(A2)}$$

A set of rules is developed to automatically classify the circling flight. For the classification of each location, five consecutive estimates of climb rate and flight direction are used; the estimates on the location itself (P_i), the two previous locations (P_{i-1} and P_{i-2}), and the next two locations (P_{i+1} and P_{i+1}). Three criteria are used for the classification of circling flight: 1) The change between the different flight directions at the five locations must be larger than 180°. 2) The average climb rate at the five locations must be positive. 3) The ground speed of the bird must be larger than 5 m s^{-1}. If the sequence of five locations satisfies all three criteria, location P_i is classified as circling flight.

Estimation of sink rate. The sink rate of a soaring bird relative to air can be estimated based on an equation by Pennycuick (1971), where sink rate is a function of horizontal airspeed and morphological characteristics:

$$V_s = \frac{2kW}{\pi \rho_0 b^2 V} + \frac{C_{D_0} \rho_0 S V^3}{2W}, \quad \text{(A3)}$$

where W is the weight (N) of the individual, b is the wing span (m), S is the wing area (m^2), ρ_0 is the air density at sea level (kg m^{-3}), and k and C_{d_0} are species-dependent coefficients [k is a drag coefficient related to the efficiency of the wings in producing lift, and C_{d_0} is a zero-lift drag coefficient, which is related to the size and shape of the bird (Welch et al. 1977)]. The airspeed of the bird V (m s^{-1}) is estimated in the current study by subtracting the drift velocity of a thermal, as an estimate of the wind speed, from the ground speed of the bird during the climb phase as measured by the GPS.

The turning motion, which is needed to stay in a thermal column, causes an inclined position of the bird's wings relative to the horizontal. The angle depends on the radius of the circles and the horizontal velocity and is typically between 20° and 40° (Pennycuick 1971). This influences the sink rate of a circling bird V_{sc}, which is a little bit higher than the sink rate in straight gliding flight. This difference is estimated with

$$V_{sc} = \frac{V_s}{\sqrt{\cos^3 \phi}}, \quad \text{(A4)}$$

where ϕ is the bank angle (Shannon et al. 2002b). The bank angle is estimated with

$$\phi = \sin^{-1} \frac{V^2}{rg}, \quad \text{(A5)}$$

where r is the turning radius (m) and g is the gravitational acceleration 9.81 m s^{-2}.

The sink rate is mainly sensitive to variations in the airspeed of the bird. Estimates for white-backed vultures, which are very similar to griffon vultures, yield $k = 1$ and $C_{d_0} = 0.0232$ (Pennycuick 1971). The mass of a griffon vulture is highly variable as it is able to fast for long periods and can eat up to 1.5 kg of meat in one feed. Average body mass is estimated per individual from measured head and beak sizes, which are correlated to body mass. The wing spans and wing areas of the griffon vultures have not been measured directly; however, the folded wings have been measured. On another set of captive griffon vultures measurements are done of wing span, wing area, and folded wing, where these variables are found to be highly correlated. This makes it possible to roughly estimate wing span and wing area from the folded wing measurements. An overview of the characteristics of the four vultures used in this research is shown in Table A1.

Table A1. Characteristics of four griffon vultures from the population in the Grands Causses area. GPS data from these vultures was collected on 2 Aug 2012. The parameters mass, wing span, and wing area are used to estimate the sink rate of the vulture relative to air.

Individual	Sex	Age (yr)	Mass (kg)	Wing span (m)	Wing area (m^2)
212	Female	17	7.99	2.54	0.972
224	Female	5	8.27	2.52	0.953
226	Female	6	8.92	2.56	0.986
730	Female	16	7.86	2.59	1.012

REFERENCES

Berens, P., 2009: CircStat: A MATLAB toolbox for circular statistics. *J. Stat. Software*, **31**, 1–21, doi:10.18637/jss.v031.i10.

Bohrer, G., and Coauthors, 2012: Estimating updraft velocity components over large spatial scales: Contrasting migration strategies of golden eagles and turkey vultures. *Ecol. Lett.*, **15**, 96–103, doi:10.1111/j.1461-0248.2011.01713.x.

Bouten, W., E. Baaij, J. Shamoun-Baranes, and K. Camphuysen, 2013: A flexible GPS tracking system for studying bird behaviour at multiple scales. *J. Ornithol.*, **154**, 571–580, doi:10.1007/s10336-012-0908-1.

Charrassin, J., and Coauthors, 2008: Southern Ocean frontal structure and sea-ice formation rates revealed by elephant seals. *Proc. Natl. Acad. Sci. USA*, **105**, 11 634–11 639, doi:10.1073/pnas.0800790105.

Dee, D. P., and Coauthors, 2011. The ERA-Interim reanalysis: configuration and performance of the data assimilation system. *Quart. J. Roy. Meteor. Soc.*, **137**, 553–597, doi:10.1002/qj.828.

Dodge, S., and Coauthors, 2013: The environmental-data automated track annotation (*Env-DATA*) system: Linking animal tracks with environmental data. *Mov. Ecol.*, **1** (3), 1–14, doi:10.1186/2051-3933-1-3.

——, and Coauthors, 2014: Environmental drivers of variability in the movement ecology of turkey vultures *(Cathartes aura)* in North and South America. *Philos. Trans. Roy. Soc. London*, **369B**, doi:10.1098/rstb.2013.0195.

Dragon, A., P. Monestiez, A. Bar-Hen, and C. Guinet, 2010: Linking foraging behaviour to physical oceanographic structures: Southern elephant seals and mesoscale eddies east of Kerguelen Islands. *Prog. Oceanogr.*, **87**, 61–71, doi:10.1016/j.pocean.2010.09.025.

Duriez, O., A. Kato, C. Tromp, G. Dell'Omo, A. Vyssotski, F. Sarrazin, and Y. Ropert-Coudert, 2014: How cheap is soaring flight in raptors? A preliminary investigation in freely-flying vultures. *PloS ONE*, **9**, e84887, doi:10.1371/journal.pone.0084887.

EEA, 2006: Corine land cover types. European Environment Agency, accessed 30 October 2012. [Available online at www.eea.europa.eu/data-and-maps.]

Hedenstrom, A., 1993: Migration by soaring or flapping flight in birds: The relative importance of energy cost and speed. *Philos. Trans. Roy. Soc. London*, **342B**, 353–361, doi:10.1098/rstb.1993.0164.

Huffaker, E., 1898: *On Soaring Flight.* U.S. Government Printing Office, 48 pp.

Kerlinger, P., 1989: *Flight Strategies of Migrating Hawks.* University of Chicago Press, 392 pp.

——, and S. Gauthreaux, 1984: Flight behaviour of sharp-shinned hawks during migration. I: Over land. *Anim. Behav.*, **32**, 1021–1028, doi:10.1016/S0003-3472(84)80216-X.

Lanzone, M., and Coauthors, 2012: Flight responses by a migratory soaring raptor to changing meteorological conditions. *Biol. Lett.*, **8**, 710–713, doi:10.1098/rsbl.2012.0359.

Lenschow, D., and P. Stephens, 1980: The role of thermals in the convective boundary layer. *Bound.-Layer Meteor.*, **19**, 509–532, doi:10.1007/BF00122351.

Mahoney, W., III, and J. O'Sullivan, 2013: Realizing the potential of vehicle-based observations. *Bull. Amer. Meteor. Soc.*, **94**, 1007–1018, doi:10.1175/BAMS-D-12-00044.1.

Mandel, J., K. Bildstein, G. Bohrer, and D. Winkler, 2008: Movement ecology of migration in turkey vultures. *Proc. Natl. Acad. Sci. USA*, **105**, 19 102–19 107, doi:10.1073/pnas.0801789105.

——, G. Bohrer, D. Winkler, D. Barber, C. Houston, and K. Bildstein, 2011: Migration path annotation: Cross-continental study of migration-flight response to environmental conditions. *Ecol. Appl.*, **21**, 2258–2268, doi:10.1890/10-1651.1.

Mass, C., and L. Madaus, 2014: Surface pressure observations from smartphones: A potential revolution for high-resolution weather prediction? *Bull. Amer. Meteor. Soc.*, **95**, 1343–1349, doi:10.1175/BAMS-D-13-00188.1.

Monsarrat, S., S. Benhamou, F. Sarrazin, C. Bessa-Gomes, W. Bouten, and O. Duriez, 2013: How predictability of feeding patches affects home range and foraging habitat selection in avian social scavengers? *PloS ONE*, **8**, e53077, doi:10.1371/journal.pone.0053077.

NASA, 2012: Srtm 90. CGIAR Consortium for Spatial Information, accessed 26 October 2012. [Available online at http://srtm.csi.cgiar.org.]

Nathan, R., W. M. Getz, E. Revilla, M. Holyoak, R. Kadmon, D. Saltz, and P. E. Smouse, 2008: A movement ecology paradigm for unifying organismal movement research. *Proc. Natl. Acad. Sci. USA*, **105**, 19 052–19 059, doi:10.1073/pnas.0800375105.

Pennycuick, C., 1971: Gliding flight of the white-backed vulture *Gyps africanus. J. Exp. Biol.*, **55**, 13–38.

Ropert-Coudert, Y., and R. Wilson, 2005: Trends and perspectives in animal-attached remote sensing. *Front. Ecol. Environ.*, **3**, 437–444, doi:10.1890/1540-9295(2005)003[0437:TAPIAR]2.0.CO;2.

Rutz, C., and G. Hays, 2009: New frontiers in biologging science. *Biol. Lett.*, **5**, 289–292, doi:10.1098/rsbl.2009.0089.

Safi, K., and Coauthors, 2013: Flying with the wind: Scale dependency of speed and direction measurements in

modelling wind support in avian flight. *Mov. Ecol.*, **1**, 10–1186, doi:10.1186/2051-3933-1-4.

Sakamoto, K. Q., A. Takahashi, T. Iwata, T. Yamamoto, M. Yamamoto, and P. Trathan, 2013: Heart rate and estimated energy expenditure of flapping and gliding in black-browed albatrosses. *J. Exp. Biol.*, **216**, 3175–3182, doi:10.1242/jeb.079905.

Santoso, E., and R. Stull, 2001: Similarity equations for wind and temperature profiles in the radix layer, at the bottom of the convective boundary layer. *J. Atmos. Sci.*, **58**, 1446–1464, doi:10.1175/1520-0469(2001)058<1446:SEFWAT>2.0.CO;2.

Sapir, N., N. Horvitz, M. Wikelski, R. Avissar, Y. Mahrer, and R. Nathan, 2011: Migration by soaring or flapping: Numerical atmospheric simulations reveal that turbulence kinetic energy dictates bee-eater flight mode. *Proc. Roy. Soc.*, **278B**, 3380–3386, doi:10.1098/rspb.2011.0358.

Shamoun-Baranes, J., A. Baharad, P. Alpert, P. Berthold, Y. Yom-Tov, Y. Dvir, and Y. Leshem, 2003a: The effect of wind, season and latitude on the migration speed of white storks *Ciconia ciconia*, along the eastern migration route. *J. Avian Biol.*, **34**, 97–104, doi:10.1034/j.1600-048X.2003.03079.x.

——, Y. Leshem, Y. Yom-Tov, and O. Liechti, 2003b: Differential use of thermal convection by soaring birds over central Israel. *Condor*, **105**, 208–218, doi:10.1650/0010-5422(2003)105[0208:DUOTCB]2.0.CO;2.

——, W. Bouten, and E. van Loon, 2010: Integrating meteorology into research on migration. *Integr. Comp. Biol.*, **50**, 280–292, doi:10.1093/icb/icq011.

——, ——, C. Camphuysen, and E. Baaij, 2011: Riding the tide: Intriguing observations of gulls resting at sea during breeding. *Ibis*, **153**, 411–415, doi:10.1111/j.1474-919X.2010.01096.x.

Shannon, H., G. Young, M. Yates, M. Fuller, and W. Seegar, 2002a: American white pelican soaring flight times and altitudes relative to changes in thermal depth and intensity. *Condor*, **104**, 679–683, doi:10.1650/0010-5422(2002)104[0679:AWPSFT]2.0.CO;2.

——, ——, ——, ——, and ——, 2002b: Measurements of thermal updraft intensity over complex terrain using American white pelicans and a simple boundary-layer forecast model. *Bound.-Layer Meteor.*, **104**, 167–199, doi:10.1023/A:1016095804357.

Shepard, E., S. Lambertucci, D. Vallmitjana, and R. Wilson, 2011: Energy beyond food: Foraging theory informs time spent in thermals by a large soaring bird. *PloS ONE*, **6**, e27375, doi:10.1371/journal.pone.0027375.

——, R. Wilson, W. Rees, E. Grundy, S. Lambertucci, and S. Vosper, 2013: Energy landscapes shape animal movement ecology. *Amer. Nat.*, **182**, 298–312, doi:10.1086/671257.

Spaar, R., and B. Bruderer, 1996: Soaring migration of steppe eagles *Aquila nipalensis* in southern Israel: Flight behaviour under various wind and thermal conditions. *J. Avian Biol.*, **27**, 289–301, doi:10.2307/3677260.

Stull, R., 1988: *An Introduction to Boundary Layer Meteorology*. Atmospheric and Oceanographic Sciences Library, Vol. 13, Springer, 670 pp.

Tucker, V., 1987: Gliding birds: The effect of variable wing span. *J. Exp. Biol.*, **133**, 33–58.

Van Loon, E., J. Shamoun-Baranes, W. Bouten, and S. Davis, 2011: Understanding soaring bird migration through interactions and decisions at the individual level. *J. Theor. Biol.*, **270**, 112–126, doi:10.1016/j.jtbi.2010.10.038.

Vansteelant, W., W. Bouten, R. Klaassen, B. Koks, A. Schlaich, J. van Diermen, E. Van Loon, and J. Shamoun-Baranes, 2014: Regional and seasonal flight speeds of soaring migrants and the role of weather conditions at hourly and daily scales. *J. Avian Biol.*, **46**, 25–39, doi:10.1111/jav.00457.

Walko, R., and R. Avissar, 2008: The Ocean–Land–Atmosphere Model (OLAM). Part I: Shallow-water tests. *Mon. Wea. Rev.*, **136**, 4033–4044, doi:10.1175/2008MWR2522.1.

Welch, A., L. Welch, and F. G. Irving, 1977: *New Soaring Pilot*. John Murray Publishers, 412 pp.

Woodcock, A., 1940: Convection and soaring over the open sea. *J. Mar. Res.*, **3**, 248–253.

AMS titles now available as eBooks at springer.com

AMS BOOKS

RESEARCH APPLICATIONS HISTORY

www.ametsoc.org/amsbookstore

Springer

Scan to see AMS eBook titles at springer.com

AMERICAN METEOROLOGICAL SOCIETY